A method to deal with installation errors of wearable accelerometers for human activity recognition

2011 Physiol. Meas. 32 347

(http://iopscience.iop.org/0967-3334/32/3/006)

IOP PUBLISHING PHYSIOLOGICAL MEASUREMENT

Physiol. Meas. **32** (2011) 347–358 doi:10.1088/0967-3334/32/3/006

A method to deal with installation errors of wearable accelerometers for human activity recognition

Ming Jiang[1], Hong Shang[2,4], Zhelong Wang[1,3], Hongyi Li[3] and Yuechao Wang[3]

[1] School of Control Science and Engineering, Dalian University of Technology, Dalian, Liaoning, People's Republic of China
[2] Technical Division, National Earthquake Response Support Service, Beijing, People's Republic of China
[3] Shenyang Institute of Automation, Chinese Academy of Science, Shenyang, Liaoning, People's Republic of China

E-mail: shong660@163.com (Hong Shang)

Received 11 September 2010, accepted for publication 20 January 2011
Published 18 February 2011
Online at stacks.iop.org/PM/32/347

Abstract
Human activity recognition (HAR) by using wearable accelerometers has gained significant interest in recent years in a range of healthcare areas, including inferring metabolic energy expenditure, predicting falls, measuring gait parameters and monitoring daily activities. The implementation of HAR relies heavily on the correctness of sensor fixation. The installation errors of wearable accelerometers may dramatically decrease the accuracy of HAR. In this paper, a method is proposed to improve the robustness of HAR to the installation errors of accelerometers. The method first calculates a transformation matrix by using Gram–Schmidt orthonormalization in order to eliminate the sensor's orientation error and then employs a low-pass filter with a cut-off frequency of 10 Hz to eliminate the main effect of the sensor's misplacement. The experimental results showed that the proposed method obtained a satisfactory performance for HAR. The average accuracy rate from ten subjects was 95.1% when there were no installation errors, and was 91.9% when installation errors were involved in wearable accelerometers.

Keywords: human activity recognition, accelerometer, installation error, calibration, Gram–Schmidt orthonormalization

(Some figures in this article are in colour only in the electronic version)

1. Introduction

Accelerometry offers a practical method of objectively monitoring human movements, and has particular applicability to the monitoring of free-living subjects (Mathie *et al* 2004). In recent

[4] Author to whom any correspondence should be addressed.

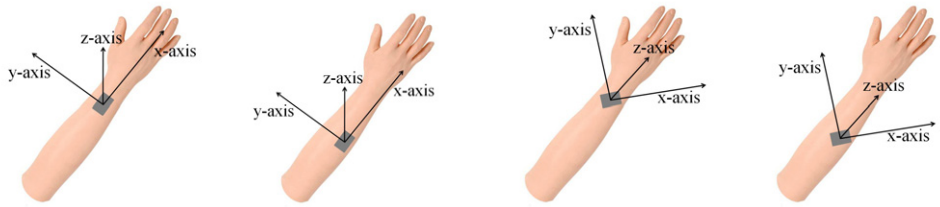

Figure 1. An arm-mounted accelerometer. (a) No installation error. (b) Misplacement. (c) Orientation error. (d) Both installation errors.

years, accelerometers have played an important role in many healthcare applications, including inferring metabolic energy expenditure (Crouter *et al* 2006, Bonomi *et al* 2009), predicting falls (Lindemann *et al* 2005, Bourke *et al* 2007), measuring gait parameters (Mayagoitia *et al* 2002, Wang *et al* 2007), and monitoring daily activities (Karantois *et al* 2006, Chen *et al* 2008, Zhang *et al* 2008, Wang *et al* 2010). Existing research works have shown that human activity recognition (HAR) by using wearable accelerometers could effectively improve the quality of healthcare provided to patients, as well as be used as a means of observing the changes of lifestyle and behavior for healthy subjects (Atallah *et al* 2010). Compared with video-based monitoring systems, the benefits of using wearable accelerometers include the following: they are of small size, have low cost, testing is not restricted to a settled environment, and they can be easily integrated with existing platforms for sensor networks (Preece *et al* 2009).

A limitation of using wearable accelerometers for HAR is that it heavily relies on the correctness of sensor installation. Because acceleration signals produced from an accelerometer are related to the sensor's orientation and placement (Mathie *et al* 2004), wearable accelerometers must be mounted on a user's body very carefully to fit the standard installation forms. In many real scenarios, it is difficult for subjects to remember the detailed orientation and placement of each body-worn accelerometer, especially when the number of accelerometers is large. If an accelerometer is mounted incorrectly due to forgetfulness or carelessness of a user, the recognition model which has already been trained to distinguish different activities will lose its effectiveness. Suppose that the standard installation form of an arm-mounted accelerometer is illustrated in figure 1(a). The misplacement of the accelerometer can be illustrated in figure 1(b). In such a case, the accelerometer is mounted in the standard orientation, but misplaced at a wrong attachment point. The orientation error can be illustrated in figure 1(c). In such a case, the accelerometer is mounted at the standard attachment point, but in a wrong orientation. Usually, both kinds of installation errors occur simultaneously, as illustrated in figure 1(d).

Some studies have been carried out to improve the robustness of HAR to the installation errors of wearable accelerometers. Zappi *et al* (2007) investigated the implications of using classifier fusion techniques to perform HAR from a number of accelerometers distributed on the body in terms of robustness to orientation errors. The experimental results showed that this method might achieve a desirable performance when the deviation angle of an accelerometer was smaller than 60°. Moreover, many additional sensors had to be used for carrying out this method. Kunze and Lukowicz (2008) presented a set of heuristics which significantly increased the robustness of sensor-based HAR. In their study, an accelerometer and a gyroscope were integrated to conquer the misplacement of inertial sensors. The experimental results showed that with certain limits and modest quality degradation, HAR could be implemented in a

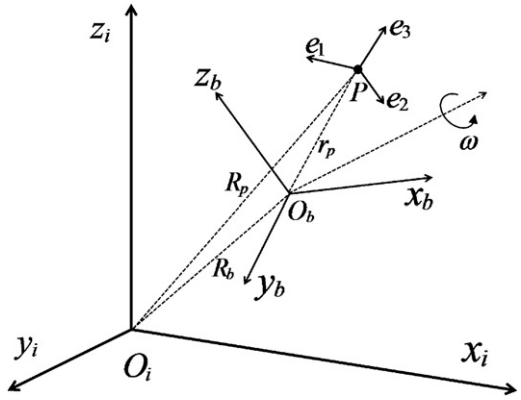

Figure 2. Geometry of an inertial frame, a body frame, and an accelerometer frame.

misplacement tolerant way. Thiemjarus (2010) described an orientation-independent method for HAR based on reference coordinate transformation. The three-dimensional acceleration signals were transformed by using a transformation matrix derived based on the known orientation of the device.

The primary limitation of the aforementioned methods is that their implementation has to use supplementary information from additional accelerometers, gyroscopes or prior knowledge, which are hard to be acquired in many real scenarios. Moreover, these methods attempted to eliminate only orientation errors or only misplacements of on-body accelerometers for HAR, but usually both kinds of installation errors occur simultaneously. In this study, a method is proposed to improve the robustness of HAR to both kinds of installation errors by using only a small number of accelerometers. The proposed method first generates a 3×3 transformation matrix to eliminate the orientation errors. The matrix is calculated by carrying out Gram–Schmidt orthonormalization to two vectors which are generated from acceleration signals of two human postures. The proposed method then reduces the main effect of the accelerometer's misplacement by implementing a low-pass filter. Finally, the support vector machine (SVM) classifier is adopted to distinguish different human activities from the calibrated acceleration signals. The organization of this paper is as follows: a detailed introduction of the proposed method is presented in section 2; an experiment for HAR is described in section 3; the experimental results are given in section 4; some discussions on the error-tolerant ability of the proposed method are made in section 5; a conclusion is drawn in section 6.

2. Materials and methods

2.1. Formulation of acceleration signals produced from a wearable accelerometer

A common approximation used in this study is that a human body can be regarded as small rigid bodies connected by joints. A rigid body can be regarded as an ideal solid body of finite size, where the relative position of any two given points remains constant. Each rigid body, such as a forearm or a shank, is allowed to rotate around one axis or more. To describe the motion of a rigid body, consider an earth-centered inertial frame $O_i x_i y_i z_i$, a body frame $O_b x_b y_b z_b$ and a point P on the moving rigid body, as shown in figure 2. Using $O_i x_i y_i z_i$, any

object may get a unique coordinate vector to describe its location in three-dimensional space (Cardou and Angeles 2009). The body frame $O_b x_b y_b z_b$ has its origin at the center of a rigid body and has its coordinate axes along the fixed directions of the rigid body. The acceleration of point P can be formulated by (Chen *et al* 1994)

$$a = \ddot{R}_b + \ddot{r}_p + \dot{\omega} \times r_p + 2\omega \times \dot{r}_p + \omega \times (\omega \times r_p) + g \tag{1}$$

where $\ddot{R}_b$ represents the translational acceleration of point O_b relative to point O_i, $\ddot{r}_p$ represents the translational acceleration of point P relative to point O_b, ω is the angular velocity of $O_b x_b y_b z_b$, the operator $\times$ denotes the cross-product operation, the term $\dot{\omega} \times r_p$ represents the tangential acceleration owing to the angular acceleration of the rotating frame $O_b x_b y_b z_b$, the term $2\omega \times \dot{r}_p$ is known as the Coriolis acceleration, the term $\omega \times (\omega \times r_p)$ represents a centripetal acceleration, and g denotes the gravitational acceleration. If point P is fixed in the moving rigid body (like the case in this study), the terms $\ddot{r}_p$ and $\dot{r}_p$ vanish (Chen *et al* 1994).

Let e_1, e_2 and e_3 denote the sensing directions of a tri-axial accelerometer mounted at point P as shown in figure 2. Because e_1, e_2 and e_3 are mutually orthogonal, they form an accelerometer frame $Pe_1e_2e_3$. The transformation matrix $\theta = (e_1, e_2, e_3)$ may map vectors from $O_i x_i y_i z_i$ to $Pe_1e_2e_3$. Thus, the acceleration signals produced from an accelerometer can be formulated by

$$A = \theta \cdot [\ddot{R}_b + \dot{\omega} \times r_p + \omega \times (\omega \times r_p) + g]. \tag{2}$$

2.2. Method to calibrate signals from an accelerometer with orientation errors

In this section, consider that there are only orientation errors, just like the case illustrated in figure 1(c).

2.2.1. Impact of orientation errors on the acceleration signals. If an accelerometer is mounted in a wrong orientation, its sensing directions are changed. Let $\hat{e}_1$, $\hat{e}_2$ and $\hat{e}_3$ denote the changed sensing directions, the accelerometer frame is changed to $P\hat{e}_1\hat{e}_3\hat{e}_3$ and the transformation matrix is changed to $\hat{\theta} = (\hat{e}_1, \hat{e}_2, \hat{e}_3)$. In this case, the acceleration signals can be formulated by

$$\hat{A} = \hat{\theta} \cdot [\ddot{R}_b + \dot{\omega} \times r_p + \omega \times (\omega \times r_p) + g]. \tag{3}$$

To calibrate the acceleration signals $\hat{A}$, the rotation matrix $N = \theta \cdot \hat{\theta}^{-1}$ which transforms vectors from $P\hat{e}_1\hat{e}_3\hat{e}_3$ to $Pe_1e_2e_3$ according to the following equation should be known:

$$A = N \cdot \hat{A}. \tag{4}$$

A common way to define a rotation matrix between two frames is by using Euler angles (Biedenharn *et al* 1981), which represent three composed rotations that move a reference frame ($P\hat{e}_1\hat{e}_3\hat{e}_3$) to a given referred frame ($Pe_1e_2e_3$). Given three Euler angles α, β and γ which denote the angles of rotating $P\hat{e}_1\hat{e}_3\hat{e}_3$ about e_1, e_2 and e_3, respectively, the rotation matrix can be formulated by

$$N = \begin{bmatrix} c_2c_3 & s_1s_2c_3 - c_1s_3 & c_1s_2c_3 + s_1s_3 \\ c_2s_3 & s_1s_2s_3 + c_1c_3 & c_1s_2s_3 - s_1c_3 \\ -s_2 & s_1c_2 & c_1c_2 \end{bmatrix} \tag{5}$$

where c_1, c_2 and c_3 denote $\cos\alpha$, $\cos\beta$ and $\cos\gamma$, respectively, and s_1, s_2 and s_3 denote $\sin\alpha$, $\sin\beta$ and $\sin\gamma$, respectively. Note that once an accelerometer is fixed on a rigid body, its orientation keeps unchanged with respect to the orientation of the rigid body. This means that

the orientation of the frame $P\hat{e}_1\hat{e}_3\hat{e}_3$ relative to the frame $Pe_1e_2e_3$ is also unchanged. Thus, the three Euler angles α, β and γ are constant and N is also constant. Name N a calibration matrix in this paper.

2.2.2. Calculation of a calibration matrix using Gram–Schmidt orthonormalization. To calculate a calibration matrix according to (5), three Euler angles must be found. Unfortunately, it is theoretically not possible to accurately measure these angles by using only one accelerometer. In this study, a method based on Gram–Schmidt orthonormalization is used to calculate a calibration matrix. The Gram–Schmidt process is a method for orthonormalizing a set of vectors in an inner product space (Trefethen and Bau 1997). Suppose that there are two acceleration vectors h_1 and h_2 obtained from an accelerometer mounted in the standard orientation. If h_1 and h_2 are non-collinear, an orthogonal matrix $M = (r_1, r_2, r_3)$ can be generated by using the Gram–Schmidt process formulated as follows:

$$\begin{cases} r_1 = \alpha_1/\|\alpha_1\|, & \alpha_1 = h_1 \\ r_2 = \alpha_2/\|\alpha_2\|, & \alpha_2 = h_2 - \langle h_2, r_1\rangle \cdot r_1 \\ r_3 = r_1 \times r_2 \end{cases} \tag{6}$$

where the operator $\|\cdot\|$ denotes Euclidean norm operation, and the operator $\langle\cdot,\cdot\rangle$ denotes inner-product operation. According to (4), the corresponding acceleration vectors obtained from an accelerometer mounted in a wrong orientation can be formulated as $\hat{h}_j = N^{-1} \cdot h_j$ $(j = 1, 2)$. Let $\hat{M}$ denote the orthogonal matrix derived from $\hat{h}_1$ and $\hat{h}_2$ according to (6). Thus, the calibration matrix N can be calculated by

$$N = M \cdot \hat{M}^{-1}. \tag{7}$$

According to the characters of an orthogonal matrix, the inverse matrix $\hat{M}^{-1}$ in (7) can be replaced by a transposed matrix $\hat{M}^T$ to reduce the amount of calculation.

To make the calculation more reliable, h_j and $\hat{h}_j$ $(j = 1, 2)$ are generated by averaging the output signals of two human postures for a second or two. Name these postures calibration postures in this paper. The calibration process is described as follows.

(1) When an accelerometer is mounted on a user's body at the first time, its mounted orientation is defined as the standard orientation.
(2) A user performs two different postures defined as calibration postures to acquire h_j $(j = 1, 2)$, and an orthogonal matrix M is calculated according to (6).
(3) Whenever the accelerometer is re-mounted, a user repeats the calibration postures to acquire $\hat{h}_j$ $(j = 1, 2)$, and the other orthogonal matrix $\hat{M}$ is calculated.
(4) A calibration matrix is then calculated according to (7), and the acceleration signals can be calibrated according to (4).

The calculation of a calibration matrix using Gram–Schmidt orthonormalization includes two main advantages. Firstly, the implementation is quite simple and convenient. Only four acceleration vectors generated from two simple human postures are needed, avoiding the use of additional sensors and expensive computation of Euler angles. Secondly, the Gram–Schmidt process has a good error-tolerant ability for calculating a calibration matrix. The calibration results may keep high accuracy when a user performs low-accuracy calibration postures. A detailed discussion on the error-tolerant ability is given in section 5.

2.3. Method to calibrate signals from a misplaced accelerometer

In this section, consider that an accelerometer is mounted in the standard orientation but misplaced at the wrong attachment point, just like the case illustrated in figure 1(b). Let the

wrong attachment point be represented by $\tilde{P}$. Let $r_{\tilde{p}}$ denote the position vector of $\tilde{P}$ with respect to the center of a rigid body. According to (2), acceleration signals produced from the misplaced accelerometer can be formulated by

$$\tilde{A} = \theta \cdot [\ddot{R}_b + \dot{\omega} \times r_{\tilde{p}} + \omega \times (\omega \times r_{\tilde{p}}) + g]. \tag{8}$$

Note that only the acceleration due to rotation is sensitive to the sensor's misplacement. The acceleration due to translation and gravity is independent of the sensor's placement. A naive idea of calibrating acceleration signals is to remove the rotational part, which is formulated as $\dot{\omega} \times r_{\tilde{p}}$ and $\omega \times (\omega \times r_{\tilde{p}})$ in (8), from the signals. Unfortunately, by using just one accelerometer, it is theoretically not possible to separate acceleration signals into rotational, translational and gravitational parts, and further eliminate the rotational part.

An acceptable solution is to reduce the main effect of the sensor's misplacement as far as possible. For most activities of daily lives, the movement of a human body is basically slow and with moderate fluctuation, so any strong acceleration is likely to last no longer than a few tenths of a second. By contrast, the acceleration due to gravity, which is predominantly contained in the low-frequency part of the acceleration signals, often remains unchanged for seconds. Moreover, for accelerometers mounted close to a joint of an arm or a leg, the output signals are dominated by the gravitational signals (Kern *et al* 2003). Because acceleration due to gravity is independent of the sensor's placement, low-pass filtered acceleration signals, which are dominated by gravity, are basically tolerant of the sensor's misplacement.

In this study, a low-pass filter with a cut-off frequency of 10 Hz is designed to remove high-frequency components from the acceleration signals. Among a range of trials, the impact of selection of low-pass filters on the calibration results is insignificant. In this study, a zero-phase Chebyshev type II infinite impulse response (IIR) low-pass filter is adopted for its simple design, high computational efficiency and short delays. The use of zero-phase filtering may effectively overcome the nonlinear phase shift caused by the IIR filters. It should be emphasized that other low-pass filters, such as finite impulse response (FIR) filters, may also work for the proposed method.

2.4. Method to recognize human activities by using acceleration data

HAR by using acceleration data may generally be divided into three steps (Preece *et al* 2009). Firstly, acceleration data are segmented into small time segments as observation windows, and each window corresponds to an activity. In this study, a sliding window technique is adopted to cut acceleration data into windows with the same length. There is also a 50% overlap between adjacent windows to avoid information loss at the boundary of windows. Secondly, some features are extracted from a window to characterize an activity. In this study, the extracted features include mean, variance, correlation, magnitudes of fast Fourier transform (FFT) coefficients and energy. These features are selected because they have already shown their efficiency of representing the characteristics of human activities (Bao and Intille 2004). The energy feature is calculated as the sum of the squared magnitudes of FFT coefficients. Finally, feature vectors are used as inputs of a classifier which associate each window with an activity. In this study, the SVM classifier is adopted to distinguish human activities due to its high recognition accuracy and strong generalization ability proved in previous studies (Lau *et al* 2008, Yin *et al* 2008). A diagram of the proposed method is shown in figure 3.

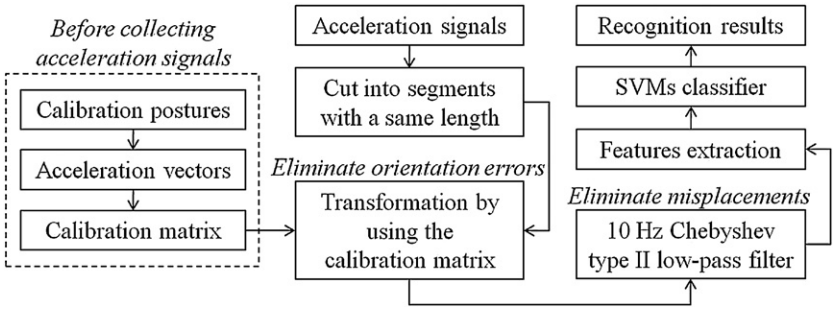

Figure 3. Diagram of the proposed method.

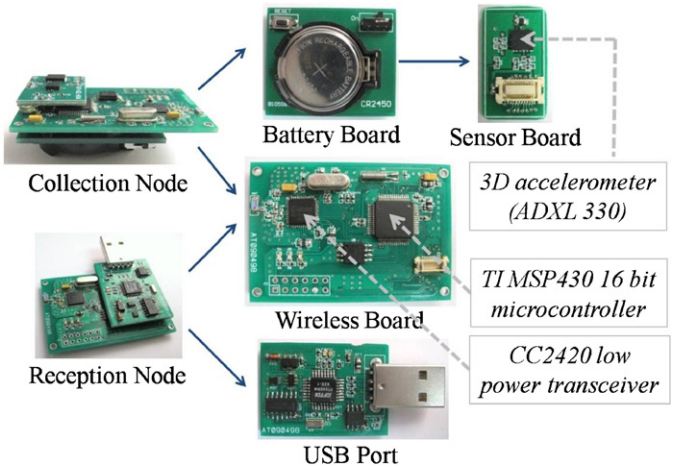

Figure 4. Configuration of the collection node and the reception node.

3. Experiment

3.1. Introduction of the experiment platform

The experiment platform used in this study was established based on body sensor networks (BSNs). The platform consisted of signal collection nodes and signal reception nodes. Each collection node consisted of a sensor board, a wireless communication board and a battery board. Each reception node consisted of a wireless communication board and a USB port. Configuration of the two nodes is shown in figure 4. Each sensor board included a tri-axial accelerometer (ADXL330) which could measure acceleration with a minimum full-scale range of ± 3 g. Each wireless communication board ran TinyOS on a microcontroller (MSP430) and communicated by using a wireless transceiver chip (CC2420) with the IEEE 802.15.4 protocol (ZigBee). The receiving frequency of acceleration signals was set at 20 Hz in this study, which might achieve a minimal packet loss.

Table 1. Recognition results of each activity.

Label	S1	S2	L	W1	J	C	W2	R1	R2	W3	Accuracy (%)
S1	473	3	2	0	0	0	0	0	0	0	99.0
S2	6	480	1	0	0	0	0	0	0	0	98.6
L1	4	5	469	0	0	0	0	0	0	0	98.1
W1	0	0	0	450	3	9	18	0	2	0	93.4
J	0	0	0	7	452	11	5	9	0	0	93.4
C	0	0	0	6	16	448	12	10	0	8	89.6
W2	0	0	0	9	0	7	453	8	1	0	94.8
R1	0	0	0	11	8	12	9	438	0	0	91.6
R2	0	0	0	2	0	0	2	0	462	14	96.3
W3	0	0	0	0	0	1	0	0	17	458	96.2

3.2. Data collection

The experiment was performed in a laboratorial environment where a clear definition of each activity and accurate labels could be provided. Ten subjects (6 males, 4 females; age 24 ± 3 years) took part in this experiment. Each subject mounted four accelerometers (collection nodes) on his/her left forearm, right forearm, left shank and right shank, respectively. Detailed attachment point and orientation of each accelerometer could be determined by the subjects. After installation, each subject was first asked to perform a range of calibration postures. The calibration postures were holding each arm/leg vertically and horizontally for 2 s. Then each subject was asked to perform ten daily activities and gym exercises, including 'standing straight' (S1), 'sitting on a chair' (S2), 'lying on a bed' (L), 'walking' (W1), 'jogging' (J), 'cycling' (C), 'walking on an elliptical machine' (W2), 'running on an elliptical machine' (R1), 'rowing' (R2) and 'weight lifting' (W3). The duration of each activity was about 120 s. After performing all activities, each subject re-mounted all body-worn accelerometers to make sure that the fixed positions and orientations were different from the previous ones. After re-installation, each subject repeated the calibration postures and the ten activities.

4. Results

4.1. Performance of the SVM classifier

For each subject, 90% of the acceleration data collected at the first time were used to train a SVM classifier. The length of sliding windows was selected to be 128 samples (about 6 s), which was long enough to describe human activities. The 128-sample length also enabled fast computation of FFT. The rest 10% of the acceleration data were used to test the performance of the trained SVM classifier. The testing results of all ten subjects are listed in table 1, where the labels in columns denote the true activities, and the labels in rows denote the recognition results. As listed in table 1, the recognition accuracy rate was high for all activities (95.1% in average). This suggested that the performance of the trained SVM classifier was quite well when there were no installation errors.

Table 2. Recognition accuracy rate of each activity (%).

	S1	S2	L	W1	J	C	W2	R1	R2	W3
Case 1	57.5	64.9	65.6	79.2	80.3	83.0	77.1	82.1	83.9	78.3
Case 2	96.2	97.2	97.0	88.9	87.6	87.4	90.4	90.8	89.8	86.7
Case 3	96.2	97.2	97.0	90.2	88.3	90.0	89.2	90.8	91.6	88.9

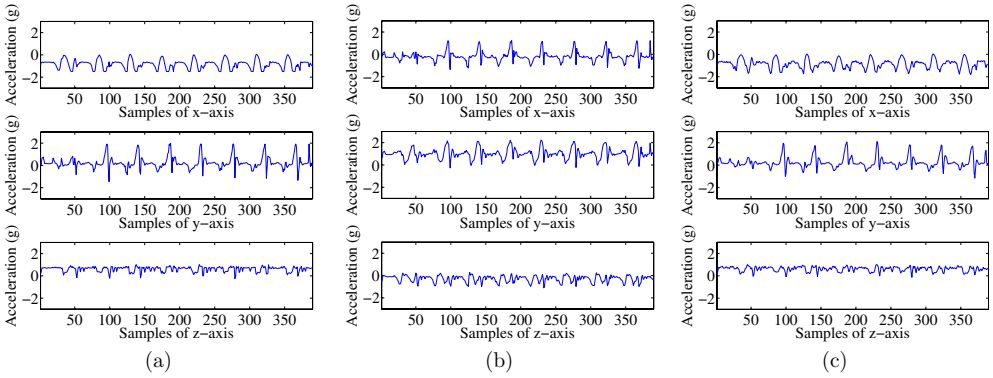

Figure 5. A period of 'cycling' signals produced from a left-shank-mounted accelerometer. (a) No installation error. (b) Both installation errors. (c) After eliminating orientation errors.

4.2. Performance of the proposed calibration method

Firstly, the performance of the trained SVM classifier was tested once more by using the acceleration data collected at the second time. In this case, the accelerometer data were polluted by installation errors. The recognition accuracy rate of each activity is listed in table 2 (case 1), which decreased dramatically (74.5% in average) compared with the corresponding results listed in table 1. This proved that the reliability of HAR heavily depended on the correctness of sensor installation.

Secondly, the proposed method was carried out to eliminate only the orientation errors included in the testing dataset (acceleration data collected at the second time). The recognition accuracy rate of each activity in this case is listed in table 2 (case 2), which was quite improved (91.2% in average). Figures 5(a) and (b) show a period of 'cycling' signals collected at the first time and at the second time, respectively. It could be found that the waveforms in figure 5(b) were quite different from the waveforms in figure 5(a). Figure 5(c) shows the calibrated 'cycling' signals. It could be found that the difference between figures 5(c) and (a) was quite small after eliminating the orientation errors.

Finally, the proposed method was carried out to eliminate both kinds of installation errors included in the testing dataset. The recognition accuracy rate of each activity in this case is listed in table 2 (case 3). The recognition accuracy rate of most activities was further improved (91.9% in average). It could also be found that the improvement was quite minor. This is because for most activities performed in this study, the acceleration signals are basically dominated by translational and gravitational acceleration which are independent of the sensor's placement. In fact, for many daily activities, sometimes just ignoring the sensor's misplacement can be enough for the misplacement tolerant recognition.

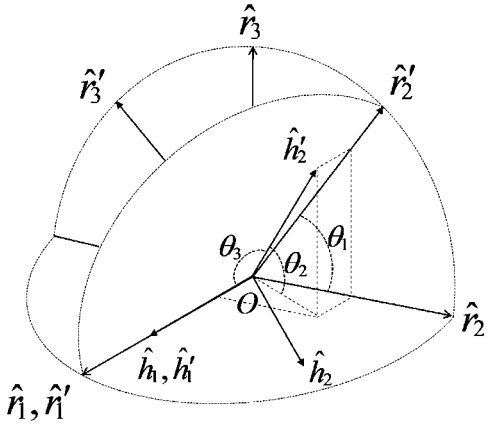

Figure 6. The geometrical relationship between $(\hat{r}_1, \hat{r}_2, \hat{r}_3)$ and $(\hat{r}_1', \hat{r}_2', \hat{r}_3')$.

5. Discussion

In order to take into account orientation errors, a user should repeat two postures to generate two acceleration vectors for calculating a calibration matrix. In some actual situations, it is hard for a user to exactly repeat a posture. The differences of performing a same posture between two times may impact the calibration results. In this section, the discussion is made on how sensitive the results would be to the inaccuracy of performing calibration postures. The discussion result will show that with certain limits and appropriate selection of calibration postures, the proposed method based on Gram–Schmidt orthonormalization may achieve a good error-tolerant ability.

Let $\hat{h}_1'$ and $\hat{h}_2'$ denote vectors generated when a user repeats calibration postures inaccurately. Let $\hat{M}' = (\hat{r}_1', \hat{r}_2', \hat{r}_3')$ denote an orthogonal matrix calculated from $\hat{h}_1'$ and $\hat{h}_2'$ according to (6), and N' denote the corresponding calibration matrix calculated according to (7). The calibration error (CAER) can be defined by

$$\text{CAER} = \max_{x \in R^3} \frac{\|N \cdot x - N' \cdot x\|}{\|x\|} = \|N - N'\| \leqslant \|\hat{M} - \hat{M}'\| \cdot \|M\| \tag{9}$$

where the operator $\|\cdot\|$ also denotes the Euclidean norm operation of a matrix. Because M is invariable, the upper bound of CAER is only relative to $\hat{M}$ and $\hat{M}'$.

For the purpose of simplifying the analysis, suppose that only one calibration posture is repeated inaccurately. The supposition is reasonable because some postures are easy for a user to perform almost unchangeably at different times, like keeping arms/legs vertically in the experiment. Let $\hat{h}_1 = \hat{h}_1'$ and $\hat{h}_2 \neq \hat{h}_2'$. The geometrical relationship between $\hat{M} = (\hat{r}_1, \hat{r}_2, \hat{r}_3)$ and $\hat{M}' = (\hat{r}_1', \hat{r}_2', \hat{r}_3')$ can be illustrated in figure 6. Note that the angle between $\hat{r}_2$ and $\hat{r}_2'$ is equal to the angle between $\hat{r}_3$ and $\hat{r}_3'$. Let this angle be represented by θ_1 ($\in [0, \pi]$). Because $\|\hat{r}_i\| = \|\hat{r}_i'\| = 1$ ($i = 1, 2, 3$) according to (6), $\|\hat{M} - \hat{M}'\|$ can be formulated as

$$\|\hat{M} - \hat{M}'\| = \sqrt{\sum_{i=1}^{3} \|\hat{r}_i - \hat{r}_i'\|^2} = 2\sqrt{2} \left| \sin \frac{\theta_1}{2} \right| = 2\sqrt{1 - \cos\theta_1}. \tag{10}$$

So, as $\cos\theta_1$ increases, CAER decreases. Let the angle between $\hat{h}_2'$ and $\hat{h}_1\hat{h}_2$ plane be represented by θ_2 ($\in [0, \pi/2]$), and the angle between $\hat{h}_2'$ and $\hat{h}_1$ be represented by θ_3 ($\in [0, \pi]$). Let the coordinate values of vector $\hat{h}_2'$ in frame $O\hat{r}_1\hat{r}_2\hat{r}_3$ be represented by

(a_1, a_2, a_3). The formulas $(\cos\theta_1)^2 = a_2^2/(a_2^2 + a_3^2)$, $(\sin\theta_2)^2 = a_3^2/(a_1^2 + a_2^2 + a_3^2)$ and $(\sin\theta_3)^2 = (a_2^2 + a_3^2)/(a_1^2 + a_2^2 + a_3^2)$ hold. So $\cos\theta_1$ can be formulated as

$$|\cos\theta_1| = \sqrt{\frac{a_2^2}{a_2^2 + a_3^2}} = \sqrt{1 - \frac{a_3^2}{a_2^2 + a_3^2}} = \sqrt{1 - \frac{\sin^2\theta_2}{\sin^2\theta_3}} \tag{11}$$

where $\cos\theta_1$ is nonnegative when $\hat{h}_2$ and $\hat{h}_2'$ are on the same side of the $\hat{r}_1\hat{r}_3$ plane, and $\cos\theta_1$ is negative otherwise.

Note that when $\cos\theta_1$ is nonnegative, $\cos\theta_1$ increases as $\sin\theta_2$ decreases, and $\cos\theta_1$ increases as $\sin\theta_3$ increases. According to (10) and (11), if $\theta_2 = 0^\circ$, CAER is vanished regardless of θ_3, and if $\theta_3 = 90^\circ$, CAER depends only on θ_2. This means that even if the difference between $\hat{h}_2'$ and $\hat{h}_2$ is large, CAER may still be very small so long as θ_2 is close to 0° and θ_3 is close to 90°. Thus, so long as the inaccurately repeated posture is mainly parallel to the plane of the two standard calibration postures, which may make a small θ_2, the calibration results are almost not interfered. Furthermore, if the two standard calibration postures are selected to be mutually orthogonal, just like the case in this study, it is more likely for the inaccurately repeated posture to make a small θ_3 to reduce the CAER further. Therefore, with simple limits and careful selection of calibration postures, the proposed calibration method based on Gram–Schmidt orthonormalization may achieve a good error-tolerant ability.

6. Conclusion

In this paper, a method is proposed to deal with the installation errors of body-worn accelerometers for HAR. This method may effectively improve the robustness of HAR to both misplacement and orientation errors of wearable accelerometers without using additional sensors and prior knowledge. In the proposed method, a calibration matrix which is calculated based on Gram–Schmidt orthonormalization is used to eliminate the orientation errors, and a low-pass filter with a cut-off frequency of 10 Hz is employed to remove the main effect of the sensor's misplacement. A SVM classifier is finally implemented to recognize human activities by using the calibrated acceleration data. The experimental results have shown that the proposed method may obtain a satisfactory performance for HAR. The average recognition accuracy rate was 95.1% when there were no installation errors, and was 91.9% when both kinds of installation error existed and polluted acceleration signals. Moreover, by using Gram–Schmidt orthonormalization, the calibration results may keep high accuracy when a user performs low-accuracy calibration postures.

Acknowledgments

This work was partially supported by National High Technology Research and Development Program 863 grant no 2007AA041502, China Postdoctoral Science Foundation grant no 20080441102, and China Earthquake Research Funds grant no 200808075.

References

Atallah L, Lo B, King R and Yang G Z 2010 Sensor placement for activity detection using wearable accelerometers *Proc. 2010 Int. Conf. on Body Sensor Networks* pp 24–9

Bao L and Intille S 2004 Activity recognition from user-annotated acceleration data *Pervasive Computing (Lecture Notes in Comput. Science* vol 3001*)* (Berlin: Springer-Verlag) pp 1–17

Biedenharn L C, Louck J G and Carruthers P A 1981 *Angular Momentum in Quantum Physics: Theory and Application* (Reading, MA: Addison-Wesley)

Bonomi A G, Plasqui G, Goris A H C and Westerterp K R 2009 Improving assessment of daily energy expenditure by identifying types of physical activity with a single accelerometer *J. Appl. Physiol.* **107** 655–61

Bourke A K, O'Brien J V and Lyons G M 2007 Evaluation of threshold-based tri-axial accelerometer fall detection algorithm *Gait and Posture* **26** 194–9

Cardou P and Angeles J 2009 Linear estimation of the rigid-body acceleration field from point-acceleration measurements *J. Dyn. Systems, Meas. Control* **131** 041013

Chen J H, Lee S C and DeBra D B 1994 Gyroscope free strapdown inertial measurement unit by six linear accelerometers *J. Guid. Control Dyn.* **17** 286–90

Chen Y P, Yang J Y, Liou S N, Lee G Y and Wang J S 2008 Online classifier construction algorithm for human activity detection using a tri-axial accelerometer *Appl. Math. Comput.* **205** 849–60

Crouter S, Clowers K and Bassett D J 2006 A novel method for using accelerometer data to predict energy expenditure *J. Appl. Physiol.* **100** 1324–31

Karantois D M, Narayanan M R, Mathie M, Lovell N H and Celler B G 2006 Implementation of a real-time human movement classifier using a triaxial accelerometer for ambulatory monitoring *IEEE Trans. Inf. Technol. i Biomed.* **10** 156–67

Kern N, Schiele B, Junker H, Lukowicz P and Tröster G 2003 Wearable sensing to annotate meeting recordings *Pers. Ubiquitous Comput.* **7** 263–74

Kunze K and Lukowicz P 2008 Dealing with sensor displacement in motion-based onbody activity recognition systems *Proc. 10th Int. Conf. on Ubiquitous Computing* pp 20–9

Lau H Y, Tong K Y and Zhu H 2008 Support vector machine for classification of walking conditions using miniature kinematic sensors *Med. Biol. Eng. Comput.* **46** 563–73

Lindemann U, Hock A, Stuber M, Keck W and Becker C 2005 Evaluation of a fall detector based on accelerometers: a pilot study *Med. Biol. Eng. Comput.* **43** 548–51

Mathie M J, Coster A C F, Lovell N H and Celler B G 2004 Accelerometry: providing an integrated, practical method for long-term, ambulatory monitoring of human movement *Physiol. Meas.* **25** R1–20

Mayagoitia R E, Lotters J C, Veltink P H and Hermens H 2002 Standing balance evaluation using a triaxial accelerometer *Gait and Posture* **16** 55–9

Preece S J, Goulermas J Y, Kenney L P J, Howard D, Meijer K and Crompton R 2009 Activity identification using body-mounted sensors—a review of classification techniques *Physiol. Meas.* **30** R1–33

Thiemjarus S 2010 A device-orientation independent method for activity recognition *Proc. 2010 Int. Conf. on Body Sensor Networks* pp 19–23

Trefethen L N and Bau D 1997 *Numerical Linear Algebra* (Philadelphia, PA: SIAM)

Wang N, Ambikairajah E, Lovell N H and Celler B G 2007 Accelerometry based classification of walking patterns using time-frequency analysis *Proc. 29th Annu. Int. Conf. of the IEEE Engineering in Medicine and Biology Society* pp 4899–902

Wang Z L, Jiang M, Zhao H Y, Li H Y and Wang Y C 2010 A pilot study on evaluating recovery of the post-operative based on acceleration and sEMG *2010 Int. Conf. on Body Sensor Networks* pp 3–8

Yin J, Yang Q and Pan J J 2008 Sensor-based abnormal human-activity detection *IEEE Trans. Knowl. Data Eng.* **20** 1082–90

Zappi P, Stiefmeier T, Farella E, Roggen D, Benini L and Troster G 2007 Activity recognition from on-body sensors by classifier fusion: sensor scalability and robustness *Proc. 3rd Int. Conf. on Intelligent Sensors, Sensor Networks and Information* pp 281–6

Zhang S, Ang Jr M H, Xiao W and Tham C K 2008 Detection of activities for daily life surveillance: eating and drinking *Proc. 10th Int. Conf. on e-Health Networking, Applications and Services* pp 171–6